Electronic and Raman Spectroscopic Properties of Oxo-Bridged Dinuclear Iron Centers in Proteins and Model Compounds

Joann Sanders-Loehr,*[1a] William D. Wheeler,[1b] Andrew K. Shiemke,[1c] Bruce A. Averill,[1d] and Thomas M. Loehr[1a]

Contribution from the Department of Chemical and Biological Sciences, Oregon Graduate Center, Beaverton, Oregon 97006-1999. *Received March 13, 1989*

Abstract: Oxo-bridged dinuclear Fe(III) complexes generally exhibit a strongly enhanced Fe–O–Fe symmetric stretching vibration in their resonance Raman spectra upon excitation into an oxo → Fe(III) charge-transfer band. The Fe–O–Fe mode has been identified in the proteins hemerythrin and ribonucleotide reductase, as well as in a number of monobridged and tribridged model compounds, from its intensity, its shift upon ^{18}O substitution, and its frequency dependence with respect to the Fe–O–Fe angle. Resonance Raman excitation profiles for the proteins and model compounds show that the Fe–O–Fe enhancement maxima tend to correspond to minor oxo → Fe(III) CT bands in the absorption spectra. The molar scattering intensity of ν_s(Fe–O–Fe) relative to $\nu_1(SO_4)$ is ~10 times greater for the proteins (with values of 300–1200) than for the model complexes (with values of 10–90). The only model compounds that were found to exhibit as great a ν_s(Fe–O–Fe) enhancement as in the proteins were the tribridged $Fe_2O(HBpz_3)_2(OAc)_2$ and $[Fe_2O(tmip)_2(OPr)_2]^{2+}$ complexes (with values of 320 and 380, respectively). These complexes have the closest structural similarity to the known dinuclear iron site in hemerythrin. Factors which elevate the intensity of the Fe–O–Fe symmetric stretch are (i) multiple bridging groups (2- to 4-fold enhancement), (ii) unsaturated nitrogen ligands cis to the oxo group (a further 2- to 4-fold enhancement), and (iii) unsaturated nitrogen ligands trans to the oxo group (additional 3- to 8-fold enhancement compared to cis ligands). The strong scattering intensity of the Fe–O–Fe mode in ribonucleotide reductase is indicative of one or two imidazole ligands trans to the oxo bridge, as in hemerythrin. Both proteins exhibit a more intense ν_{as}(Fe–O–Fe) than is observed with symmetric model complexes; this suggests that the two metal atoms in each dinuclear iron center are not equivalent.

Oxo-bridged dinuclear Fe(III) complexes are well-known products of aqueous iron chemistry that have been extensively studied by spectroscopic, magnetic, and structural techniques.[2,3] Interest in these compounds has been sparked by the discovery of a class of dinuclear iron proteins containing the Fe–O–Fe moiety.[4] Members of this class include the invertebrate respiratory protein, hemerythrin, and the enzymes ribonucleotide reductase, purple acid phosphatase, and methane monooxygenase. The oxo-bridged structure has been definitively identified in hemerythrin by X-ray crystallography[5,6] and in ribonucleotide reductase by resonance Raman spectroscopy.[7] The presence of an oxo-bridged diiron center in purple acid phosphatase has been strongly implicated by the short iron–iron distance of ~3.0 Å, the antiferromagnetic coupling of the irons, and the existence of a stable one-electron-reduced species with EPR parameters similar to semimethemerythrin.[4] However, the failure to observe a resonance-enhanced Fe–O–Fe mode in the Raman spectrum of purple acid phosphatase[8] and the lack of a short Fe–O distance in the EXAFS[9] has made it difficult to verify the presence of the Fe–O–Fe group in this protein. Consequently, we have undertaken a study of the Raman spectroscopic characteristics of the Fe–O–Fe symmetric stretch in a number of model compounds in order to determine the structural factors that influence the intensity of this vibrational mode.

Scheme I

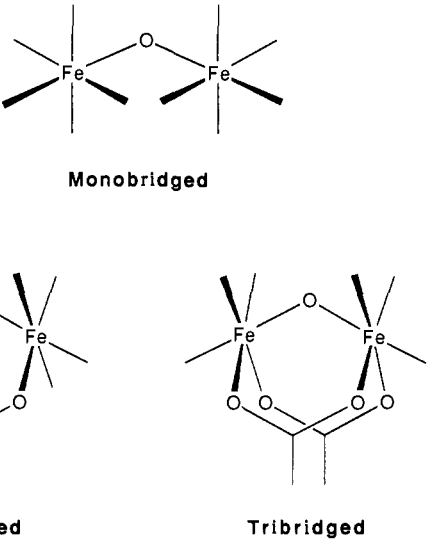

The model complexes studied fall into several categories based on the type of Fe–O–Fe core they possess. These are shown schematically below. The monobridged complexes contain two Fe(III) ions coordinated to a common oxo ion, with the remaining five-coordination sites filled with a variety of ligands ranging from bi- to pentadentate (Figure 1, a–f).[10-14b] The tribridged complexes typically have two μ-carboxylato linkages in addition to the single oxo bridge. The three remaining coordination sites on each iron

(1) (a) Oregon Graduate Center. (b) Department of Chemistry, University of Wyoming, Laramie, WY 82071. (c) Department of Chemistry, California Institute of Technology, Pasadena, CA 91125. (d) Department of Chemistry, University of Virginia, Charlottesville, VA 22901.

(2) Murray, K. S. *Coord. Chem. Rev.* **1974**, *12*, 1.

(3) Lippard, S. J. *Angew. Chem., Int. Ed. Engl.* **1988**, *27*, 344.

(4) Sanders-Loehr, J. In *Iron Carriers and Iron Proteins*; Loehr, T. M., Ed.; VCH: New York, 1989; pp 373–466.

(5) (a) Stenkamp, R. E.; Sieker, L. C.; Jensen, L. H. *J. Am. Chem. Soc.* **1984**, *106*, 618. (b) Sheriff, S.; Hendrickson, W. A.; Smith, J. L. *J. Mol. Biol.* **1987**, *197*, 273.

(6) Stenkamp, R. E.; Sieker, L. C.; Jensen, L. H.; McCallum, J. D.; Sanders-Loehr, J. *Proc. Natl. Acad. Sci. U.S.A.* **1985**, *82*, 713.

(7) (a) Sjöberg, B.-M.; Loehr, T. M.; Sanders-Loehr, J. *Biochemistry* **1982**, *21*, 96. (b) Backes, G.; Sahlin, M.; Sjöberg, B.-M.; Loehr, T. M.; Sanders-Loehr, J. *Biochemistry* **1989**, *28*, 1923.

(8) Averill, B. A.; Davis, J. C.; Burman, S.; Zirino, T.; Sanders-Loehr, J.; Loehr, T. M.; Sage, J. T.; Debrunner, P. G. *J. Am. Chem. Soc.* **1987**, *109*, 3760.

(9) (a) Kauzlarich, S. M.; Teo, B. K.; Zirino, T.; Burman, S.; Davis, J. C.; Averill, B. A. *Inorg. Chem.* **1986**, *25*, 2781. (b) Que, L., Jr.; Scarrow, R. C. In *Metal Clusters in Proteins*; Que, L., Jr., Ed.; American Chemical Society: Washington, DC, 1988; pp 152–178.

(10) Plowman, J. E.; Loehr, T. M.; Schauer, C. K.; Anderson, O. P. *Inorg. Chem.* **1984**, *23*, 3553.

(11) (a) Davies, J. E.; Gatehouse, B. M. *Cryst. Struct. Commun.* **1972**, *1*, 115. (b) Davies, J. E.; Gatehouse, B. M. *Acta Crystallogr.* **1972**, *B28*, 3541.

(12) Lippard, S. J.; Schugar, H.; Walling, C. *Inorg. Chem.* **1967**, *6*, 1825.

(13) Ou, C. C.; Wollmann, R. G.; Hendrickson, D. N.; Potenza, J. A.; Schugar, H. J. *J. Am. Chem. Soc.* **1978**, *100*, 4717.

(14) (a) Gomez-Romero, P.; DeFotis, G. C.; Jameson, G. B. *J. Am. Chem. Soc.* **1986**, *108*, 851. (b) Gomez-Romero, P.; Witten, E. H.; Reiff, W. M.; Backes, G.; Sanders-Loehr, J.; Jameson, G. B. *J. Am. Chem. Soc.*, in press. (c) Gomez-Romero, P.; Casan-Pastor, N.; Ben-Hussein, A.; Jameson, G. B. *J. Am. Chem. Soc.* **1988**, *110*, 1988. (d) Wu, F.-J.; Kurtz, D. M., Jr. *J. Am. Chem. Soc.*, in press.

0002-7863/89/1511-8084$01.50/0

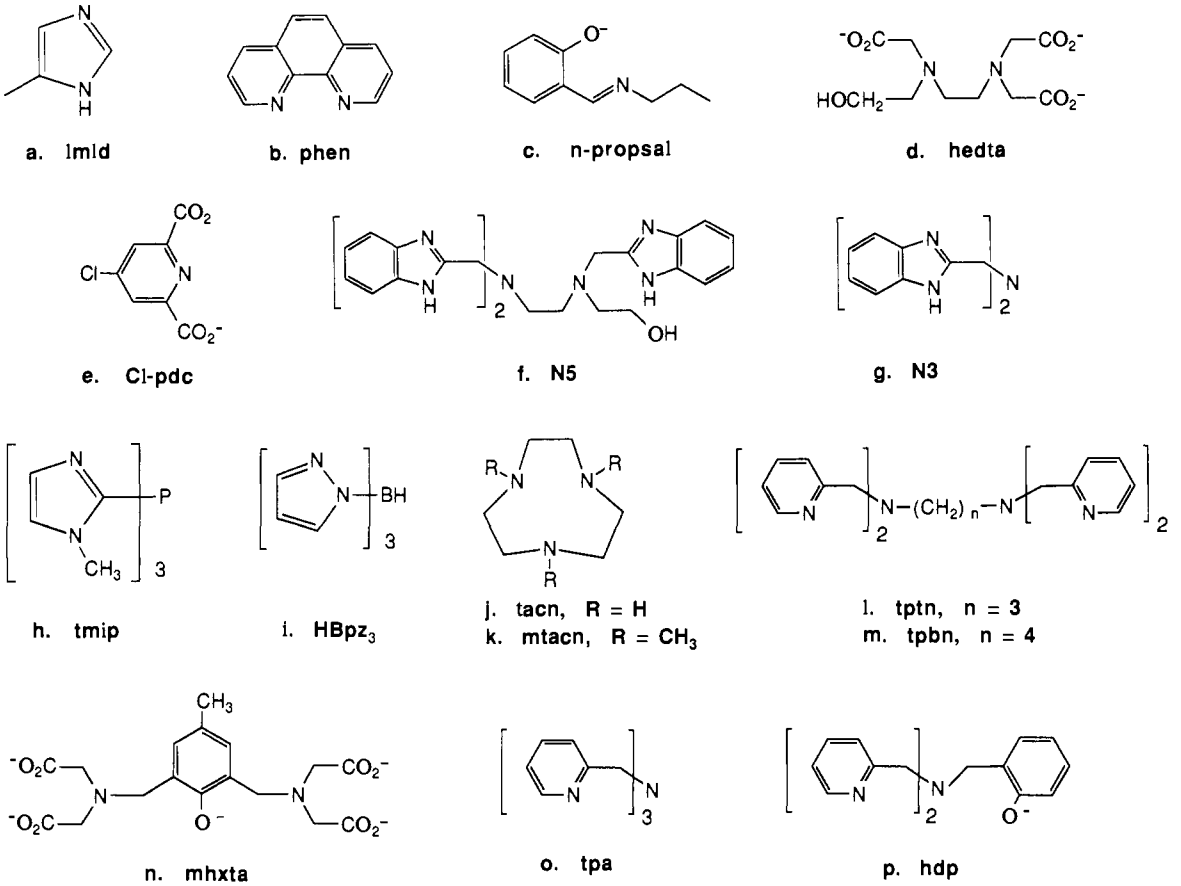

Figure 1. Principal coordinating ligands for oxo-bridged dinuclear iron complexes used in this study: (a) imidazole ligand from histidine in dinuclear iron proteins, (b) 1,10-phenanthroline, (c) *n*-propylsalicylidinimine, (d) *N*-hydroxyethylethylenediaminetriacetate, (e) 4-chloro-2,6-pyridinedicarboxylate, (f) *N*-hydroxyethyl-*N*,*N*′,*N*′-tris(2-(benzimidazolyl)methyl)ethanediamine, (g) bis(2-benzimidazolylmethyl)amine, (h) tris(*N*-methylimidazol-2-yl)-phosphine, (i) hydrotris(1-pyrazolyl)borate, (j) 1,4,7-triazacyclononane, (k) *N*,*N*′,*N*″-trimethyl-1,4,7-triazacyclononane, (l) tetrakis(2-pyridylmethyl)-1,3-propanediamine, (m) tetrakis(2-pyridylmethyl)-1,4-butanediamine, (n) *N*,*N*′-2-hydroxy-5-methyl-1,3-xylylenebis[*N*-(carboxymethyl)glycine], (o) tris(2-pyridylmethyl)amine, (p) *N*-(*o*-hydroxybenzyl)-*N*,*N*-bis(2-pyridylmethyl)amine.

are filled by a tridentate ligand (Figure 1, g–m).[14c–18] More recently, the use of tetradentate ligands (Figure 1, o, p) has led to the discovery of dibridged complexes where the two iron atoms are joined by one μ-oxo and one μ-carboxylato group.[20,21]

The tribridged complexes have a high degree of structural homology with hemerythrin. Both oxy- and methemerythrins contain a tribridged core with a solvent-derived oxo bridge and protein-derived μ-carboxylato bridges from aspartate and glutamate.[5] One Fe(III) has its remaining coordination sites filled by the imidazole side chains of three histidines, whereas the second Fe(III) is coordinated to two histidines and an exogenous anion. In this study, the hemerythrins used for comparison have azide, cyanide, cyanate, and thiocyanate (met forms) or hydroperoxide (oxy form) coordinated as the exogenous ligands. In addition, we present data for the proteins ribonucleotide reductase and purple acid phosphatase.

Oxo-bridged Fe(III) complexes exhibit intense absorption in the visible and near-UV region. Excitation within or near these absorption bands results in resonance Raman spectra that are dominated by the Fe–O–Fe symmetric stretching vibration, ν_s(Fe–O–Fe).[22] In contrast, the asymmetric stretching vibration, ν_{as}(Fe–O–Fe), is more readily observed in the infrared spectrum. Although the electronic spectra of the dinuclear iron complexes appear to be quite similar in both the wavelength and the intensity of their absorption maxima, we have found that Raman intensities for ν_s(Fe–O–Fe) show considerable variability.

Furthermore, the Raman excitation profiles for the ν_s(Fe–O–Fe) mode often fail to correspond to the principal absorption maxima. Such results have been reported previously for azidomethemerythrin[22b] and the $[Fe_2O(HBpz_3)_2(OAc)_2]$ complex.[23] These observations have led to the question of whether the intense near-UV absorption maxima can be assigned as oxo → Fe(III) charge transfer (CT)[24] or whether they might be due to some other phenomenon such as a simultaneous pair excitation of ligand-field transitions on the two iron atoms.[25] A more thorough investigation of a series of hemerythrin derivatives and model compounds has led to the conclusion that the intense near-UV features that

(15) Armstrong, W. H.; Lippard, S. J. *J. Am. Chem. Soc.* **1983**, *105*, 4837.
(16) Wieghardt, K.; Pohl, K.; Gebert, W. *Angew. Chem., Int. Ed. Engl.* **1983**, *22*, 727.
(17) Chaudhuri, P.; Wieghardt, K.; Nuber, B.; Weiss, J. *Angew. Chem., Int. Ed. Engl.* **1985**, *24*, 778.
(18) Toftlund, H.; Murray, K. S.; Zwack, P. R.; Taylor, L. F.; Anderson, O. P. *J. Chem. Soc., Chem. Commun.* **1986**, 191.
(19) Murch, B. P.; Bradley, F. C.; Boyle, P. D.; Papaefthymiou, V.; Que, L., Jr. *J. Am. Chem. Soc.* **1987**, *109*, 7993.
(20) (a) Yan, S.; Cox, D. D.; Pearce, L. L.; Juarez-Garcia, C.; Que, L., Jr.; Zhang, J. H.; O'Connor, C. J. *Inorg. Chem.*, in press. (b) Yan, S.; Norman, R. E.; Que, L., Jr.; Backes, G.; Ling, J.; Sanders-Loehr, J.; Zhang, J. H.; O'Connor, C. J., manuscript submitted.
(21) Yan, S.; Que, L., Jr.; Taylor, L. F.; Anderson, O. P. *J. Am. Chem. Soc.* **1988**, *110*, 5222.
(22) (a) Loehr, T. M.; Shiemke, A. K. In *Biological Applications of Raman Spectroscopy*; Spiro, T. G., Ed.; Wiley: New York, 1988; Vol. 3, pp 439–490. (b) Shiemke, A. K.; Loehr, T. M.; Sanders-Loehr, J. *J. Am. Chem. Soc.* **1984**, *106*, 4951.
(23) Czernuszewicz, R. S.; Sheats, J. E.; Spiro, T. G. *Inorg. Chem.* **1987**, *26*, 2063.
(24) Solomon, E. I.; Wilcox, D. E. In *Magneto-Structural Correlations in Exchange Coupled Systems*; Willett, R. D., Gatteschi, D., Kahn, O., Eds.; D. Reidel: Hingham, MA, 1985; p 463.
(25) (a) Schugar, H. J.; Rossman, G. R.; Barraclough, C. G.; Gray, H. B. *J. Am. Chem. Soc.* **1972**, *94*, 2683. (b) Schugar, H. J.; Rossman, G. R.; Thibeault, J.; Gray, H. B. *Chem. Phys. Lett.* **1970**, *6*, 26. (c) Schugar, H. J.; Hubbard, A. T.; Anson, F. C.; Gray, H. B. *J. Am. Chem. Soc.* **1969**, *91*, 71.

dominate the spectra of all oxo-bridged dinuclear Fe(III) complexes should be designated as oxo → Fe(III) CT transitions.[26] Both the variable Raman intensities and the unusual enhancement maxima for the Fe–O–Fe symmetric stretch can be interpreted within this framework.

Experimental Procedures

Model Compounds. The following compounds were generously provided for use in this study (the ligands are depicted in Figure 1): $[Fe_2O(phen)_4(H_2O)_2]Cl_4$,[10] Thomas M. Loehr; $Fe_2O(n\text{-propsal})_4$,[11a] $Fe(n\text{-propsal})_2Cl$,[11b] and $(enH_2)[Fe_2O(hedta)_2]\cdot 6H_2O$,[12] Bruce A. Averill; $Fe_2O(Cl\text{-}pdc)_2(H_2O)_4$,[13] Harvey J. Schugar; $[Fe_2O(N5)Cl_3]Cl$,[14a] $[Fe_2O(N5)Br_3]Br$,[14a,b] and $[Fe_2O(N3)_2(OBz)_2](ClO_4)_2\cdot 2C_2H_5OH\cdot 0.5(Et_3NHClO_4)$,[14c] Geoffrey B. Jameson; $[Fe_2O(tmip)_2(OPr)_2](PF_6)_2\cdot CH_3CN$,[14d] Donald M. Kurtz, Jr.; $[Fe_2O(HBpz_3)_2(OAc)_2]\cdot 0.5CH_3CN$,[15] Stephen J. Lippard; $[Fe_2O(tacn)_2(OAc)_2]I_2\cdot 3H_2O\cdot 0.5NaI$[16] and $[Fe_2O(mtacn)_2(OAc)_2](PF_6)_2$,[17] Karl Wieghardt; $[Fe_2O(tpbn)(OAc)_2]_2(NO_3)_4\cdot 4H_2O$,[18] $[Fe_2O(tpbn)(OAc)_2]_2(ClO_4)_4\cdot 4H_2O$, and $[Fe_2O(tptn)(OAc)_2]_2(NO_3)_4\cdot 4H_2O$,[18] Hans Toftlund; and $(PyrrH)_4[Fe_4O_2(mhxta)_2(OH)_2]\cdot 2CH_3OH$,[19] $[Fe_2O(tpa)_2(OBz)](ClO_4)_3$,[20a] $[Fe_2O(tpa)_2(OAc)](ClO_4)_3\cdot H_2O\cdot EtOAc$,[20a] $[Fe_2O(tpa)_2\{O_2P(OPh)_2\}](ClO_4)_3$,[20b] $[Fe_2O(tpa)_2Cl_2](ClO_4)_2$,[20b] $[Fe_2O(hdp)_2(OBz)](ClO_4)$,[21] and $[Fe_2O(hdp)_2\{O_2P(OPh)_2\}](BPh_4)$,[20b] Lawrence Que, Jr.

To compare the scattering intensities of the Fe–O–Fe symmetric stretching vibration for such a diverse set of compounds, we have recorded the Raman spectra of these complexes from homogeneous mixtures of the solid complexes with Na_2SO_4. Weighed amounts of sample and Na_2SO_4 [typically 1:3 (w/w)] were mixed by grinding for 1 min with an agate mortar and pestle. Approximately 40 mg of this mixture was packed into a sample holder with a circular groove, which was then spun at ~500 rpm and subjected to laser excitation at room temperature.

^{18}O-Isotope Shifts. A sample of $(enH_2)[Fe_2O(hedta)_2]\cdot 6H_2O$ was dissolved in $H_2{}^{18}O$ at a concentration of 0.1 M. The Raman spectrum was obtained at 15 K in an Air Products Displex refrigerator and compared to a sample prepared under identical conditions in $H_2{}^{16}O$. The spectral pattern was similar to that obtained on solid samples, but peaks were 7 to 17 cm^{-1} higher in frozen solution at 15 K. The low temperature was employed because Fe–O–Fe complexes are considerably more photolabile in solution than in the solid state. For all other model compounds, isotope shifts were determined by synthesis of the complex in $H_2{}^{18}O$ or by dissolution of the complex in organic solvent containing 1–2% $H_2{}^{18}O$.

Protein Samples. Hemerythrin was purified from *Phascolopsis gouldii*, and Raman spectra were obtained in a flow cell at 5 °C on samples in 0.05 M Tris (pH 8.0) which were ~1 mM in protein and 0.2–0.3 M in Na_2SO_4.[23] Ribonucleotide reductase from *Escherichia coli* (~2 mM in met B2, ϵ_{280} = 130 000 M^{-1} cm^{-1}) was kindly provided by John Lynch and Lawrence Que, Jr. The met B2 subunit (in 0.05 M Tris-Cl, 0.2 M Na_2SO_4, pH 7.6) was examined in a capillary at 5 °C.[7b,27] Raman samples of purple acid phosphatase from beef spleen were investigated at 15 K (Displex) in 0.01 M acetate (pH 5.0) with 2 mM protein and 0.2 M Na_2SO_4.[8] Samples of the porcine purple acid phosphatase, uteroferrin (~2 mM in 0.1 M acetate, pH 4.9), were kindly provided by Philip Aisen and were also analyzed at 15 K.

Spectroscopy. Raman spectra were recorded on a computerized Jarrell-Ash spectrophotometer[28] using an RCA C31034 photomultiplier tube, an Ortec Model 9302 amplifier-discriminator, and Spectra-Physics 164-05 (Ar) and 164-01 and 2025-11 (Kr) lasers. An ~150° backscattering geometry was used for all solid samples (spinning and frozen) and for protein samples in capillaries. A 90° scattering geometry was used with the flow cell for liquid samples. Infrared and electronic absorption spectra were obtained on a Perkin-Elmer 1800 FT-IR and a Perkin-Elmer Lambda 9 spectrophotometer, respectively.

Relative Raman *scattering intensities* (at four wavelengths) were calculated as the ratio of the molar scattering intensity (*peak area*/concentration) of the Fe–O–Fe symmetric stretch to the molar scattering intensity of the sulfate symmetric stretch at ~990 cm^{-1}. Peak areas were determined by the trace and weigh method. All proteins were examined in aqueous solution in the liquid state, whereas the model compounds had to be examined in the solid state because of their instability in water. The determination of scattering intensities from solid samples is less accurate than for solution samples owing to the difficulty of achieving homogeneous mixing and the effect of grain size on the extent of light dispersion.[29] Nevertheless, the heterogeneity problem can be minimized by use of a rotating sample, and quantitative intensities have been reported for solid samples using an inorganic salt as an internal standard.[30] In the case of sodium sulfate we found that grinding crystals for 10 min with a mortar and pestle reduced the Raman scattering intensity by about 20% and that the effect was magnified by grinding with a steel ball mill (Wig-L-Bug).[31] For this reason sample grinding time was limited to 1 min, with no observable decrease in sulfate Raman intensity. Replicate samples were in good agreement with one another. It is estimated that the relative scattering intensities reported here are accurate to ±20%.

Raman *excitation profiles* were determined from a single sample at 10 or more wavelengths using a constant spectral resolution. The absence of photodecomposition with UV excitation was verified by examining samples with visible excitation after each UV experiment. Since the peak widths remained constant, the molar scattering intensity for the excitation profiles was calculated from *peak height*/concentration. Again the Fe–O–Fe symmetric stretch was measured relative to the ν_1 mode of sulfate. The molar scattering intensities shown in the excitation profiles are ~2-fold lower than the values based on peak areas because ν_s(Fe–O–Fe) has a ~2-fold greater peak width than $\nu_1(SO_4^{2-})$.

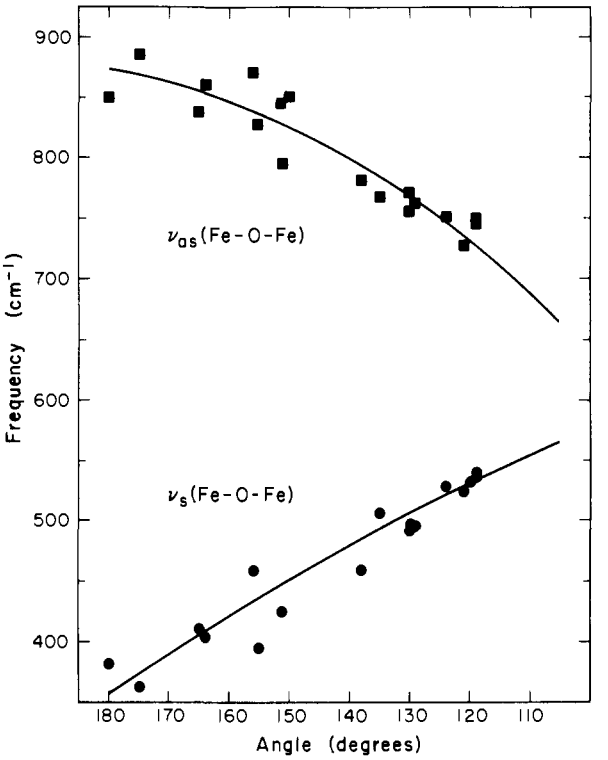

Figure 2. Correlation of vibrational frequencies for the Fe–O–Fe symmetric and asymmetric stretches with the observed Fe–O–Fe angle from Table I.

Results and Discussion

Fe–O–Fe Vibrations. The Raman and infrared spectral properties of the compounds studied are listed in Table I. In many cases ν_s(Fe–O–Fe) and ν_{as}(Fe–O–Fe) have been identified definitively by their ^{18}O isotope shifts. The energies of the two Fe–O–Fe vibrations show the expected dependence on Fe–O–Fe angle,[33] as illustrated in Figure 2. As the Fe–O–Fe angle de-

(26) Reem, R. C.; McCormick, J. M.; Richardson, D. E.; Devlin, F. J.; Stephens, P. J.; Musselman, R. L.; Solomon, E. I. *J. Am. Chem. Soc.* **1989**, *111*, 4688.
(27) Sjöberg, B.-M.; Sanders-Loehr, J.; Loehr, T. M. *Biochemistry* **1987**, *26*, 4242.
(28) Loehr, T. M.; Keyes, W. E.; Pincus, P. A. *Anal. Biochem.* **1979**, *96*, 456.
(29) Sushchinskii, M. M. *Raman Spectra of Molecules and Crystals*; Israel Program for Scientific Translations Ltd.: New York, 1972; pp 352–363.
(30) Baránska, H.; Labudzińska, A.; Terpiński, J. *Laser Raman Spectrometry. Analytical Applications*; Ellis Horwood Ltd.: Chichester, 1987; pp 161–163.
(31) Sharma, K. D., Ph.D. Dissertation, Oregon Graduate Center, 1988.
(32) Scarrow, R. C.; Maroney, M. J.; Palmer, S. M.; Que, L., Jr.; Roe, A. L.; Salowe, S. P.; Stubbe, J. A. *J. Am. Chem. Soc.* **1987**, *109*, 7857.
(33) Wing, R. M.; Callahan, K. P. *Inorg. Chem.* **1969**, *8*, 871.
(34) (a) Burke, J. M.; Kincaid, J. R.; Spiro, T. G. *J. Am. Chem. Soc.* **1978**, *100*, 6077. (b) Solbrig, R. M.; Duff, L. L.; Shriver, D. F.; Klotz, I. M. *J. Inorg. Biochem.* **1982**, *17*, 69.
(35) Spool, A.; Williams, I. D.; Lippard, S. J. *Inorg. Chem.* **1985**, *24*, 2156.

Table I. Vibrational Frequencies and Parameters of Oxo-Bridged Fe(III) Complexes

sample	Fe–O–Fe angle[a] obs	Fe–O–Fe angle[a] calc	Fe–O–Fe stretch[b] ν_s	Fe–O–Fe stretch[b] $\Delta^{18}O$	Fe–O–Fe stretch[b] ν_{as}	Fe–O–Fe stretch[b] $\Delta^{18}O$	Fe–O distances[a] Fe 1	Fe–O distances[a] Fe 2
Monobridged Complexes								
$[Fe_2O(Cl\text{-}pdc)_2(H_2O)_4]$	180		381		850		1.77	1.77
$[Fe_2O(TPP)]$	175		363		885		1.76	1.76
$[Fe_2O(hedta)_2]^{2-}$	165	167	409	−2[c]	838		1.80	1.79
$[Fe_2O(n\text{-}propsal)_4]$	164		403		860		1.76	1.78
$[Fe_2OCl_6]^{2-}$	156		458	−18	870	−44	1.76	1.76
$[Fe_2O(phen)_4(H_2O)_2]^{4+}$	155	156	395	−5	827	−39	1.78	1.78
$[Fe_4O_2(mhxta)_2(OH)_2]^{4-}$	151	152	425	−7	795		1.79	1.79
$[Fe_2O(N5)Br_5]^{+}$	151		422		846[d]		1.73	1.80
$[Fe_2O(N5)Cl_3]^{+}$	150		425		850[d]	−44	1.75	1.78
Dibridged Complexes								
$[Fe_2O(hdp)_2(OBz)]^{+}$	129	124	494	−17	763	−43	1.78	1.80
$[Fe_2O(hdp)_2(O_2PR_2)]^{+}$		148	461	−9				
$[Fe_2O(tpa)_2(OBz)]^{3+}$	130	124	497	−17	772[d]	−37	1.77	1.81
$[Fe_2O(tpa)_2(OAc)]^{3+}$	129		499		770[d]	−38	1.78	1.79
$[Fe_2O(tpa)_2(O_2PR_2)]^{3+}$	138		454		778		1.78	1.82
Tribridged Complexes								
$[Fe_2O(tacn)_2(OAc)_2]^{2+}$	119	130	540	−17	749	−33	1.78	1.78
$[Fe_2O(mtacn)_2(OAc)_2]^{2+}$	120		537				1.80	1.80
$[Fe_2O(N3)_2(OBz)_2]^{2+}$	119		537		745	−45	1.78	1.80
$[Fe_2O(tpbn)(OAc)_2]_2^{4+}$	121		525		727[d]		1.79	1.79
$[Fe_2O(tptn)(OAc)_2]_2^{4+}$			540		725			
$[Fe_2O(HBpz_3)_2(OAc)_2]$	124	128	528	−17	751	−30	1.78	1.79
$[Fe_2O(tmip)_2(OPr)_2]^{2+}$	*e*	129	533	−17[f]	749[d]	−34	*e*	*e*
Proteins								
oxyhemerythrin (HO_2^-)		134	486	−14	753	−37		
methemerythrin (N_3^-)	135	136	507	−14	768	−35	1.64	1.89
methemerythrin (SCN^-)		130	514	−16	780	−38		
methemerythrin (CN^-)		137	512	−14	782	−28		
methemerythrin (OCN^-)		143	509	−12	782	−26		
ribonucleotide reductase	130	138	493	−13	756	−25	1.78	1.78

[a] Observed Fe–O–Fe angles and Fe–O distances (in Å) from X-ray crystal structures of model compounds (references listed in Experimental Procedures) and hemerythrin (ref 5), and from EXAFS of ribonucleotide reductase (ref 32). Calculated Fe–O–Fe angles based on secular equation (ref 33) for ν_s(Fe–O–Fe) with ^{16}O and ^{18}O. [b] Frequencies in cm^{-1}. ν_s from Raman spectroscopy, ν_{as} from IR spectroscopy (model compounds), and Raman spectroscopy (proteins). Values from following sources: Cl–pdc complex ν_{as} (ref 13), TPP complex (ref 34a), hedta complex ν_{as} (ref 25a), Cl_6 complex (ref 34b), phen complex (ref 10), mhxta complex (ref 19), N5 complex (ref 14b), hdp and tpa complexes (ref 20b), tacn complex (ref 35), N3 complex ν_{as} (ref 36), tptn complex ν_{as} (ref 18), $HBpz_3$ complex (ref 37), hemerythrin complexes (ref 22), ribonucleotide reductase (ref 7b). All other values from this work. [c] Isotope shift determined for ν_s(Fe–O–Fe) at 423 cm^{-1} in aqueous solution at 15 K. [d] ν_{as} obtained from Raman spectrum. [e] Isostructural $[Fe_2O(tmip)_2(OAc)_2](ClO_4)_2$ complex has Fe–O–Fe angle of 123° and Fe–O distance of 1.80 Å (ref 14d). [f] Determined from $2\nu_s$ due to Fermi resonance of ν_s in ^{18}O sample.

creases, the frequency of the asymmetric stretch decreases while the frequency of the symmetric stretch increases. These data indicate that knowledge of ν_s and ν_{as} should allow the prediction of an Fe–O–Fe angle within 10° of the correct value.

A more accurate estimate of Fe–O–Fe angle can be obtained by comparing the Fe–O–Fe frequencies of complexes with ^{18}O and ^{16}O in the bridging position.[33] However, the magnitude of the ^{18}O effect for ν_s decreases as the Fe–O–Fe angle increases, making it particularly difficult to identify the symmetric stretch from its isotope shift as the bridge approaches linearity. Also, ^{18}O exchange is sometimes difficult to accomplish. It occurs fairly readily with ribonucleotide reductase,[7] but for oxyhemerythrin the protein must first be reduced to the ferrous state or reacted with certain anions.[22] Most of the dibridged and tribridged complexes (Table I) were found to exchange readily when a small amount of $H_2{}^{18}O$ was added to a solution of the compound in organic solvent.[20,35,37] However, all attempts to use a similar technique to accomplish ^{18}O exchange with the $[Fe_2O(tpbn)(OAc)_2]_2^{4+}$ complex led to decomposition of the sample. Thus, it is often necessary to crystallize the dinuclear iron complex from labeled solvent, as was done in the case of the $[Fe_2O(phen)_4(H_2O)_2]^{4+}$ and $[Fe_2OCl_6]^{2-}$ complexes.[10,34b]

The symmetric stretching frequencies for Fe–^{16}O–Fe and Fe–^{18}O–Fe in Table I were incorporated into a secular equation[33] from which an Fe–O–Fe angle was calculated. The results in Table I show that in cases where both crystal structure and isotope information are available, there is good agreement between the observed and calculated angles. Thus, for the majority of the model complexes, the calculated Fe–O–Fe angles are within 6° of the angles determined by X-ray crystallography. Much of the uncertainty in the calculated angle can be accounted for by the fact that vibrational frequencies are only accurate to ±1 cm^{-1}, and a 1-cm^{-1} change in ν_s(Fe–O–Fe) results in a 4–5° change in the calculated angle. The $[Fe_2OCl_6]^{2-}$ complex has an anomalously large value for the ^{18}O isotope shift, which may mean that the 458-cm^{-1} band is not a pure symmetric stretching mode (e.g., the Fe–Cl modes also exhibit ^{18}O sensitivity).[34b] Hence, calculations of the Fe–O–Fe angle would not be reliable.

Extension of the Fe–O–Fe angle calculation to molecules for which a crystal structure is not yet available yields useful information. Thus, for example, phosphato bridging as in the $[Fe_2O(hdp)_2\{O_2P(OPh)_2\}]^{+}$ complex leads to the prediction of an Fe–O–Fe angle of 148° compared to 129° for the analogous μ-carboxylato complex. In the dibridged tpa complexes (Table I) the Fe–O–Fe angle changes from 130 to 138° upon replacement of carboxylate with phosphate.[20] A related observation was made for $Fe_2O(HBpz_3)_2(OAc)_2$ versus $Fe_2O(HBpz_3)_2\{O_2P(OPh)_2\}_2$, where the Fe–O–Fe angle increased from 124° in the bis(μ-carboxylato) species to 135° in the bis(μ-phosphato) species.[38] From their ^{18}O shifts, the various derivatives of methemerythrin and oxyhemerythrin are predicted to have a common dinuclear iron structure similar to that determined crystallographically for

(36) Jameson, G. B., personal communication.
(37) Armstrong, W. H.; Spool, A.; Papaefthymiou, G. C.; Frankel, R. B.; Lippard, S. J. *J. Am. Chem. Soc.* **1984**, *106*, 3653.
(38) Armstrong, W. H.; Lippard, S. J. *J. Am. Chem. Soc.* **1985**, *107*, 3730.

azidomethemerythrin. The oxo-bridged Fe(III) site in ribonucleotide reductase must have a small Fe–O–Fe angle as well, suggesting that it also contains a carboxylato-bridged dinuclear iron site.

Use of the isotope data with the asymmetric Fe–O–Fe vibration is, however, of dubious value. The secular equation[33] for determining the Fe–O–Fe angle from isotope shifts in ν_{as}(Fe–O–Fe) is much more sensitive to peak position, and a 1-cm^{-1} change in frequency can result in a 20° change in the calculated Fe–O–Fe angle. Better results are obtained by fitting the data for ν_s and ν_{as} into a normal coordinate analysis (NCA) program utilizing the GF matrix method[39] and a general valence force field based on the method of Schachtschneider.[40] NCA calculations were performed on the Fe–O–Fe moiety of $[Fe_2O(phen)_4(H_2O)_2]^{4+}$, $[Fe_2O(tacn)_2(OAc)_2]^{2+}$, $Fe_2O(HBpz_3)_2(OAc)_2$, and azidomethemerythrin using the known Fe–O–Fe angles, the vibrational data for ν_s and ν_{as} in Table I, and assuming an Fe–O–Fe bending mode at 100 cm^{-1}.[23] Satisfactory matches to the observed frequencies for ν_s and ν_{as} were obtained with Fe–O stretching force constants of 3.2–3.4 mdyn/Å, Fe–O–Fe bending force constants of 0.1–0.2, and stretch–stretch interaction force constants of 0.2–0.6, yielding errors in calculated frequencies of 0.1–0.5%. These values are in agreement with a more detailed normal coordinate analysis which has been performed on the $Fe_2O(HBpz_3)_2(OAc)_2$ complex.[23] In that study all of the iron ligands were included in the calculations, and the 16 observed vibrational modes between 100 and 800 cm^{-1} were satisfactorily assigned.

Normal coordinate analysis calculations were also carried out for the other three methemerythrin derivatives, oxyhemerythrin, and ribonucleotide reductase. Assuming an Fe–O–Fe angle of 135° and an Fe–O bond distance of 1.80 Å gave good agreement to the observed values for ν_s(Fe–O–Fe) with errors of <0.35% and force constants similar to those for the compounds of known structure. In the case of the metcyano and metcyanato hemerythrins and ribonucleotide reductase, however, the observed oxygen isotope shift for the asymmetric stretch is anomalously small (<28 cm^{-1}). These values result in somewhat larger, but still acceptable errors of 0.7–0.9% in the calculated ν_{as}(Fe–O–Fe). Thus, NCA confirms the structural similarity of these proteins.

For the compounds in Table I for which oxygen isotope data are lacking, the Fe–O–Fe assignments have been made on the basis of peak intensities and energies expected for the known or probable Fe–O–Fe angle. A typical example is the $[Fe_2O(tpbn)(OAc)_2]_2^{4+}$ complex whose resonance Raman spectrum is shown in Figure 3. The Fe–O–Fe symmetric stretch is typically the strongest sample peak observed between 100 and 1100 cm^{-1}. On this basis, and also from the known Fe–O–Fe angle of 121° (Table I, Figure 2), the intense peak at 525 cm^{-1} is assigned to the symmetric stretch of the Fe–O–Fe core. In the upper spectrum collected with 363.8-nm excitation, there is an overtone of ν_s at 1050 cm^{-1} and a weak feature at 727 cm^{-1}, which corresponds to ν_{as} of the Fe–O–Fe moiety. The peak at 991 cm^{-1} is ν_1 of sulfate. With visible excitation (lower spectrum), several additional peaks are enhanced. The peaks between 200 and 300 cm^{-1} are probably due to Fe–N and/or Fe–O stretches of the tpbn and acetate ligands. The three bands centered at 635 cm^{-1} and two bands near 460 cm^{-1} are the triply and doubly degenerate deformation modes, respectively, of sulfate. The weak bands at 812 and 1028 cm^{-1} may be ligand modes.

In the case of the $Fe_2O(Cl\text{-}pdc)_2(H_2O)_4$ complex, the peak at 381 cm^{-1} is commensurate with the observed Fe–O–Fe angle of 180° and is also the spectral component most sensitive to excitation wavelength. Additional peaks at 431 and 457 cm^{-1} in the Cl-pdc complex shift 5–7 cm^{-1} to lower energy when the complex is prepared from D_2O and, thus, may represent vibrations of the coordinated water molecules. For $Fe_2O(n\text{-propsal})_4$ it was also not possible to accomplish ^{18}O exchange without sample decomposition. Although the Raman spectrum is dominated by phenolate ligand vibrational modes, the assignments of ν_s(Fe–O–Fe) at 403 cm^{-1} and ν_{as}(Fe–O–Fe) at 860 cm^{-1} could be made on the basis of their being at the expected frequencies for the known Fe–O–Fe angle and of their being the only two peaks not present in the Raman spectrum of the Fe(*n*-propsal)$_2$Cl monomer.

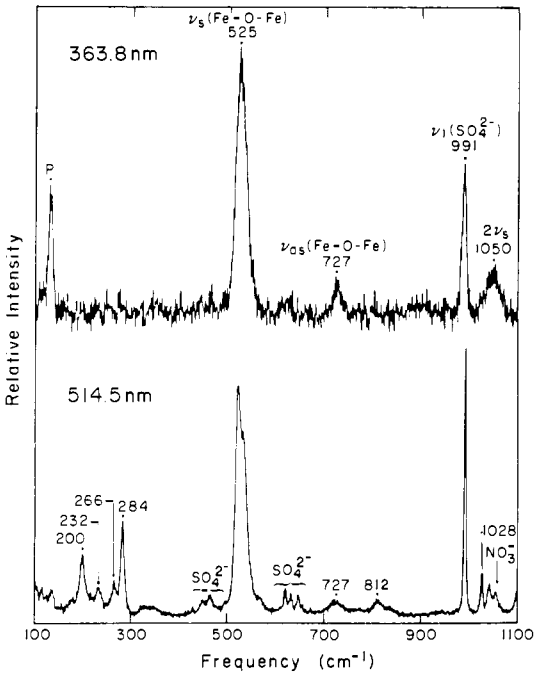

Figure 3. Resonance Raman spectra of $[Fe_2O(tpbn)(OAc)_2]_2(NO_3)_4$: upper, 363.8-nm excitation, 6 mW, 1 cm^{-1}/s, resolution 12 cm^{-1}, average of four scans; lower, 514.5-nm excitation, 50 mW, 1 cm^{-1}/s, resolution 4 cm^{-1}, average of four scans. Sample contained 12.8 mg of the complex and 32 mg of Na_2SO_4 and was spun as a solid at room temperature.

The frequency of the Fe–O–Fe symmetric stretch shows some variability when different salts of the same dinuclear iron moiety are examined. In $[Fe_2O(phen)_4(H_2O)_2]^{4+}$ complexes, for example, ν_s was found at 374 cm^{-1} in the chloride salt, at 395 cm^{-1} in the nitrate salt, and at 402 cm^{-1} in the perchlorate salt.[10] Similarly, the perchlorate salt of $[Fe_2O(tpbn)(OAc)_2]_2^{4+}$ has its ν_s at 547 cm^{-1} and $2\nu_s$ at 1095 cm^{-1}, whereas the corresponding values for the nitrate salt are at 525 cm^{-1} and 1050 cm^{-1}, respectively (Figure 3). These differences may be due to changes in Fe–O–Fe geometry caused by crystal packing forces. The frequency of the Fe–O–Fe vibration in the proteins is also sensitive to the environment. A 20- to 30-cm^{-1} decrease is observed when the oxo group is involved in hydrogen bonding, as is the case for the oxy and hydroxomet forms of hemerythrin[41] and probably also for ribonucleotide reductase.[7] Such environmental effects may account for some of the scatter of experimental points in Figure 2. An additional cause of scatter arises from vibrational energies being inversely proportional to Fe–O bond lengths.[42] While the average Fe–O distance in the di- and tribridged complexes falls between 1.78 and 1.79 Å (Table I), the values for the monobridged complexes cover a broader range of 1.76–1.80 Å and this accounts for the greater variability in their Fe–O–Fe frequencies.

Raman Enhancement Profiles. Normal modes whose vibrations coincide with a structural distortion in an electronically excited state relative to the ground state can be enhanced upon excitation into that absorption band.[43] It is expected that vibrations of an M–O–M moiety should be strongly enhanced when excited in the region of an oxo → metal CT transition.[44] In linear oxo-bridged

(39) Wilson, E. B.; Decius, J. C.; Cross, P. C. *Molecular Vibrations*; McGraw-Hill: New York, 1955.
(40) Fuhrer, H.; Kartha, V. B.; Kidd, K. G.; Krueger, P. J.; Mantsch, H. H. *Computer Programs for Infrared Spectrophotometry*; National Research Council of Canada: Ottawa, 1976; Vol. 5, Bull. No. 15.
(41) Shiemke, A. K.; Loehr, T. M.; Sanders-Loehr, J. *J. Am. Chem. Soc.* **1986**, *108*, 2437.
(42) Wieghardt, K.; Drüke, S., personal communication.
(43) (a) Spiro, T. G.; Stein, P. *Annu. Rev. Phys. Chem.* **1977**, *28*, 501. (b) Harakawa, A. Y.; Tsuboi, M. *Science* **1975**, *188*, 359. (c) Myers, A. B.; Mathies, R. A. In *Biological Applications of Raman Spectroscopy*; Spiro, T. G., Ed.; Wiley: New York, 1987; Vol. 2, pp 1–58.

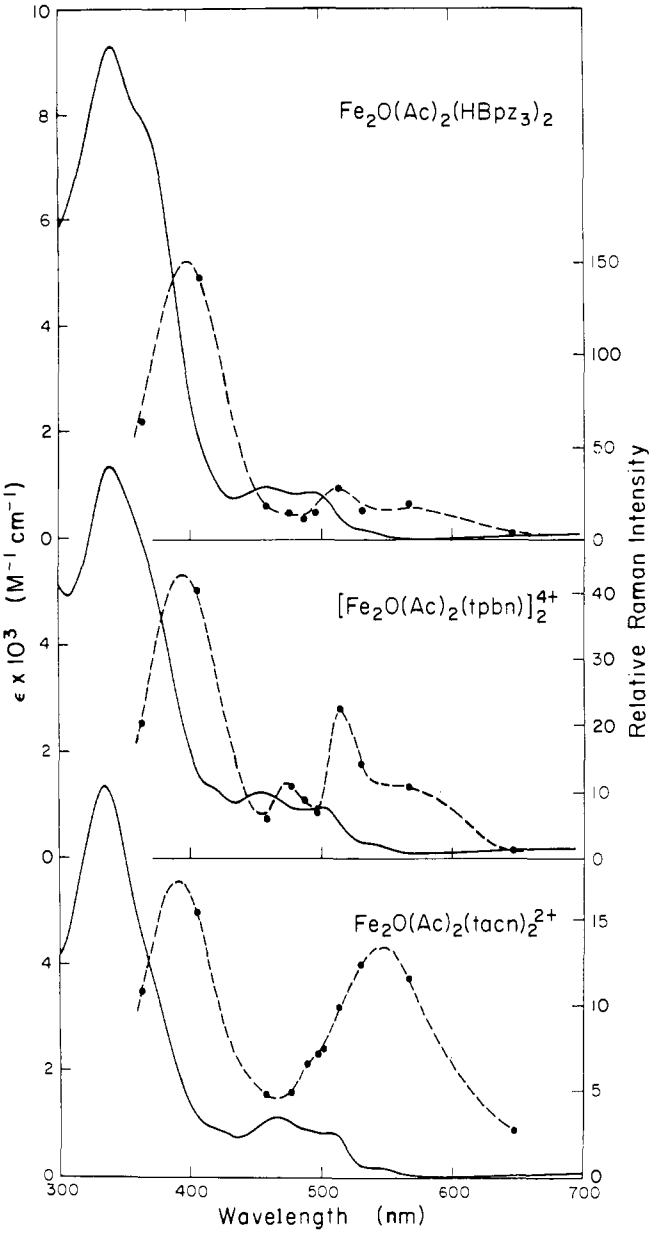

Figure 4. Resonance Raman enhancement profiles for Fe–O–Fe symmetric stretch in tribridged model compounds. Relative Raman intensity (●) calculated from the height of ν_s(Fe–O–Fe) per mole of sample relative to the height of $\nu_1(SO_4)$ per mole of sulfate. Enhancement profiles (---) drawn as a smooth curve through the data points: upper, $Fe_2O(HBpz_3)_2(OAc)_2$ peak at 528 cm^{-1}; middle, $[Fe_2O(tpbn)(OAc)_2]_2(NO_3)_4$ peak at 525 cm^{-1}; lower, $[Fe_2O(tacn)_2(OAc)_2]I_2$ peak at 540 cm^{-1}. Electronic absorption spectra (—) obtained in CH_3Cl (upper) and CH_3CN (middle and lower). Raman spectra obtained on solid samples in a spinning holder.

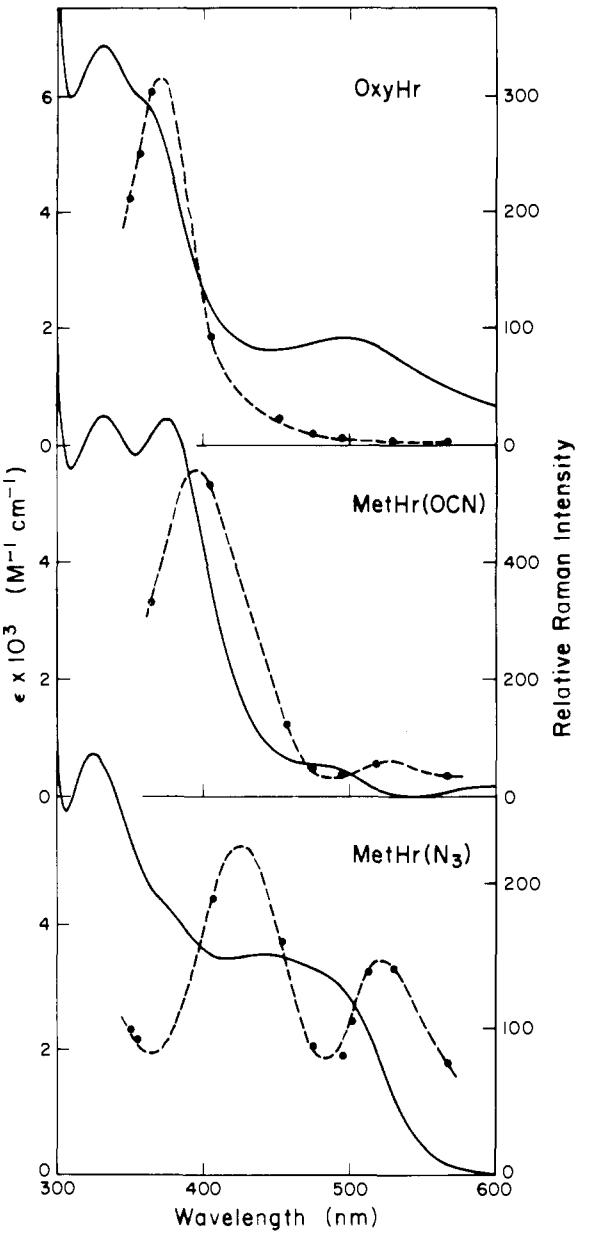

Figure 5. Resonance Raman enhancement profiles for Fe–O–Fe symmetric stretch in various forms of hemerythrin. Relative Raman intensity (---) calculated as in Figure 4 and shown in comparison to the electronic spectrum (—) with the extinction coefficient per protein monomer: upper, oxyhemerythrin peak at 486 cm^{-1}; middle, cyanatomethemerythrin peak at 509 cm^{-1}; lower, azidomethemerythrin peak at 507 cm^{-1}. Both electronic and resonance Raman spectra obtained on aqueous solutions.

dinuclear complexes of ruthenium, osmium, tungsten, and molybdenum, for example, maximal intensity of the M–O–M symmetric stretch corresponds to an intense electronic absorption band ($\epsilon \geq 5000$ M^{-1} cm^{-1}) in the visible region (400–550 nm).[45-47] Thus, an analysis of ν_s(M–O–M) enhancement as a function of excitation wavelength can help to identify electronic spectral components arising from oxo → metal CT.

Enhancement profiles for ν_s(Fe–O–Fe) have been determined for three of the tribridged model compounds (Figure 4). The Raman spectra were obtained on solid samples, mixed with sodium sulfate as an internal standard. The profile for the $Fe_2O(HBpz_3)_2(OAc)_2$ complex agrees well with that reported by Czernuszewicz et al. and obtained under similar conditions.[23] It differs somewhat in relative enhancement intensities from the one published previously for the compound dissolved in methylene chloride.[37] A considerable discrepancy in the location of excitation maxima is observed for the $[Fe_2O(tacn)_2(OAc)_2]^{2+}$ complex in the solid state (Figure 4) versus acetonitrile solution.[35] Because of the possible photodecomposition of oxo-bridged complexes in solution,[45] the Raman data obtained on solid samples in a rotating sample holder may be more reliable. Absorption spectra for the $Fe_2O(HBpz_3)_2(OAc)_2$ and $[Fe_2O(tacn)_2(OAc)_2]^{2+}$ complexes were also obtained in the solid state using KBr pellets. These were found to exhibit absorption maxima within 5 nm of the solution spectra and to have similar relative intensities of the main peaks. Thus, the comparison of solid-state excitation profiles and solution state electronic spectra in Figure 4 appears justified.

(44) Clark, R. J. H.; Stewart, B. *Struct. Bonding Berlin* **1979**, *36*, 1.
(45) San Filippo, J., Jr.; Fagan, P. J.; Di Salvo, F. J. *Inorg. Chem.* **1977**, *16*, 1016.
(46) Campbell, J. R.; Clark, R. J. H. *J. Chem. Soc., Faraday Trans. 2* **1980**, *76*, 1103.
(47) Lincoln, S. E.; Koch, S. A.; Loehr, T. M., manuscript submitted.

Table II. Electronic Spectral Data and Band Assignments for Oxo-Bridged Fe(III) Compounds

band no.	monobridged complex	tribridged complex		hemerythrin complex[d]				extinction coefficient[e]	assignment[f]
	hedta[a]	$HBpz_3$[b]	tacn[c]	Cl^-	OCN^-	HO_2^-	N_3^-		
1	235	262	275					5700–17 400	$RCO_2^- \rightarrow$ Fe CT
2	307	339	335	328	331	324	323	4500–12 800	oxo → Fe CT
3	343	358	373	384	378	370	385	3500–9300	oxo → Fe CT
4		*~400*	*~390*		*~395*		*~425*	<2000	oxo → Fe CT[g]
5	403	457	464					900–1100	$^4T_2(^4D)$ LF[h]
6						474	442	1000–2000	L → Fe CT
7						523	499	1000–2000	L → Fe CT
8	477	492	506	490	480	475		200–900	$[^4A_1{}^4E](^4G)$ LF
9		528	543	*~540*	*~530*		*~525*	~200	oxo → Fe CT[g]
10	544	695	743	656	650	750	680	80–200	$^4T_2(^4G)$ LF
11	894	995	1020	1020	1020	990	1015	5–13	$^4T_1(^4G)$ LF

[a] Values for λ_{max} in nm. Compound is $(enH_2)[Fe_2O(hedta)_2]$ in H_2O (ref 25a). [b] $Fe_2O(HBpz_3)_2(OAc)_2$ in $CHCl_3$ (ref 37). [c] $[Fe_2O(tacn)_2(OAc)_2]I_2$ in CH_3OH (ref 35). [d] Samples in H_2O. Cl^- and OCN^- derivatives (ref 26); oxy and N_3^- derivatives (ref 26, 50). [e] ϵ in M^{-1} cm^{-1} per 2 Fe. [f] Assignments taken from ref 26 and 50. CT = charge transfer; LF = ligand field transition from $^6A_1$ ground state; L = exogenous ligand. [g] Values in italics obtained from resonance Raman enhancement profiles for the symmetric Fe–O–Fe stretch (this work and ref 26 for chloromethemerythrin). [h] Band in hemerythrin obscured by LMCT transitions.

A common feature of the ν_s(Fe–O–Fe) profiles in Figure 4 is that several enhancement maxima are observed, implying that there are several electronic transitions which have oxo → Fe CT character. This has been noted previously for the tribridged $HBpz_3$ and tacn complexes.[23,35] A similar indication of multiple oxo → metal CT transitions has been reported for oxo-bridged Os(IV) and Re(IV) complexes.[45,46] Enhancement profiles for ν_s(Fe–O–Fe) in the azide and cyanate forms of methemerythrin show this same type of behavior (Figure 5). Multiple oxo → Fe CT maxima have also been reported for metchlorohemerythrin.[26]

An unusual aspect of the enhancement profiles for the dinuclear iron sites in both the tribridged models and the proteins is that the enhancement maxima tend to correspond to fairly minor features in the electronic spectra rather than to the main absorption maxima. This would imply that although the intense absorption bands are likely to arise from oxo → Fe(III) CT transitions,[26] they do not have the appropriate excited-state distortion for effective resonance enhancement of the Fe–O–Fe vibrational mode. Alternatively, the lack of agreement between the absorption maxima and the Fe–O–Fe enhancement maxima in the visible region could arise from an antiresonance phenomenon. Interference effects have been noted in certain transition metal complexes, where resonance scattering associated with both ligand field and charge-transfer transitions leads to a de-enhancement of Raman intensity in the vicinity of the LF transition and a resultant displacement of the observed enhancement maximum.[48] Although the latter explanation cannot be ruled out, the former seems more plausible in view of the observation of multiple oxo → Fe(III) CT bands in the electronic spectra of oxo-bridged dinuclear iron complexes (see below).

Assignment of Electronic Absorption Bands. As can be seen in Figures 4 and 5, the oxo-bridged dinuclear Fe(III) clusters in both proteins and model compounds exhibit surprisingly similar electronic absorption spectra.[49,50] These include two very strong bands in the near-UV region (320–380 nm) and several less intense bands in the visible region (430–550 nm). A comparison of electronic spectral components for hemerythrins and several model compounds is shown in Table II. Bands 1–3 of the monobridged hedta complex were originally assigned as simultaneous pair excitations (SPE), based on the remarkable agreement of their absorption maxima with the sums of ligand field (LF) transitions.[25] However, the polarized single-crystal absorption spectra of $(enH_2)[Fe_2O(hedta)_2]$ show that bands 1, 2, and 3 differ in their polarization characteristics.[26] Band 1 has more intensity with polarization perpendicular to the Fe–Fe axis, leading it to be assigned as a carboxylate → Fe(III) CT band. Bands 2 and 3 are considerably more intense with parallel polarization and, thus, are more likely to be due to oxo → Fe(III) CT.

The intensity of an oxo → Fe CT band in the ∥ versus ⊥ polarized absorption spectrum is expected to be a function of Fe–O–Fe angle, with more of a ⊥ component appearing as the angle deviates from a linear alignment with respect to the Fe–Fe axis. Such behavior is in fact observed. The $[Fe_2O(hedta)_2]^{2-}$ complex (Fe–O–Fe = 165°) has almost no ⊥ polarized component for band 3, whereas the hemerythrin complexes (Fe–O–Fe ≃ 135°) show ⊥ components for bands 2 and 3 ranging from 20 to 40% of the intensity of the ∥ counterparts.[26] The values approaching 40% are due to additional contributions from exogenous ligand → Fe(III) CT transitions in the ⊥ polarized spectra. A further argument in favor of an oxo → Fe(III) CT assignment as opposed to SPE is that the energy of the $^4T_2(^4G)$ LF transition in hemerythrin (band 10 in Table II) varies by 100 nm (2000 cm^{-1}) and, thus, could not combine with other LF transitions to produce SPE's (bands 2 and 3) which vary by only 15 nm (1000 cm^{-1}).[26]

The oxo → Fe(III) CT transitions in the near-UV region (bands 2 and 3) have been assigned to π overlap between p orbitals of the oxo group and d orbitals on the iron.[26] A more intense oxo → Fe CT band arising from σ orbital overlap is expected (but not yet observed) near 200 nm. The hemerythrin complexes are also likely to have LMCT transitions corresponding to carboxylate → Fe(III) CT (band 1). For example, oxyhemerythrin has an absorptivity at 280 nm of 33 000 M^{-1} cm^{-1} per subunit,[51a] which is considerably larger than the value for apohemerythrin of 23 700 M^{-1} cm^{-1} per subunit.[51b]

The two strong absorption bands in the visible region in oxo-bridged model complexes (bands 5 and 8 in Table II) can be assigned as LF transitions whose unusually high intensities ($\epsilon \leq$ 1000 M^{-1} cm^{-1}) are due in part to the relaxation of spin restrictions upon antiferromagnetic coupling of the two iron atoms.[26] Two other less intense LF transitions (bands 10 and 11) are observed in the near-IR region. A number of these LF transitions have also been identified in various forms of hemerythrin.[50] However, those in the visible region of chromophoric hemerythrins such as oxy and azidomet tend to be overshadowed by intense exogenous ligand → Fe(III) CT transitions (bands 6 and 7) from hydroperoxide and azide, respectively. The latter assignments have been verified from resonance Raman enhancement profiles for the peroxide (Fe–O and O–O) and azide (Fe–N and N–N) vibrational modes.[22b]

Enhancement profiles for the Fe–O–Fe symmetric stretch provide further information about oxo → Fe(III) CT transitions.

(48) (a) Bosworth, Y. M.; Clark, R. J. H.; Turtle, P. C. *J. Chem. Soc., Dalton Trans.* **1975**, 2027. (b) Stein, P.; Miskowski, V.; Woodruff, W. H.; Griffin, J. P.; Lerner, K. G.; Gaber, B. P.; Spiro, T. G. *J. Chem. Phys.* **1976**, *64*, 2159. (c) Schick, G. A.; Bocian, D. F. *J. Raman Spectrosc.* **1981**, *11*, 27.

(49) Garbett, K.; Darnall, D. W.; Klotz, I. M.; Williams, R. J. P. *Arch. Biochem. Biophys.* **1969**, *135*, 419.

(50) Loehr, J. S.; Loehr, T. M.; Mauk, A. G.; Gray, H. B. *J. Am. Chem. Soc.* **1980**, *102*, 6992.

(51) (a) Dunn, J. B. R.; Addison, A. W.; Bruce, R. E.; Loehr, J. S.; Loehr, T. M. *Biochemistry* **1977**, *16*, 1743. (b) Loehr, J. S.; Lammers, P. J.; Brimhall, B.; Hermodson, M. A. *J. Biol. Chem.* **1978**, *253*, 5726.

Table III. Raman Intensities of Oxo-Bridged Fe(III) Complexes

sample	rel intensity of ν_s(Fe–O–Fe) at selected excitation λ's (nm)[a] 360[c]	410[d]	458	515	intensity ratio[b] I_{as}/I_s
Monobridged Complexes					
$[Fe_2O(Cl\text{-}pdc)_2(H_2O)_4]$	25		10	5	
$[Fe_2O(hedta)_2]^{2-}$	25	20	15	5	<0.04
$[Fe_2O(n\text{-}propsal)_4]$	5	10	10	5	0.51
$[Fe_2OCl_6]^{2-}$					0.25[e]
$[Fe_2O(phen)_4(H_2O)_2]^{4+}$	25	75	70	60	0.06
$[Fe_4O_2(mhxta)_2(OH)_2]^{4-}$	<5	20	10	5	<0.04
$[Fe_2O(N5)Br_3]^+$					2.40
$[Fe_2O(N5)Cl_3]^+$	5		5	5	4.20
Dibridged Complexes					
$[Fe_2O(hdp)_2(OBz)]^+$	70	5		<1	<0.04
$[Fe_2O(hdp)_2(O_2PR_2)]^+$	50	15		10	<0.04
$[Fe_2O(tpa)_2(OBz)]^{3+}$	50	>160		70	0.33
$[Fe_2O(tpa)_2(OAc)]^{3+}$		>140		70	>0.22
$[Fe_2O(tpa)_2(O_2PR_2)]^{3+}$	100	230	65		0.18
Tribridged Complexes					
$[Fe_2O(tacn)_2(OAc)_2]^{2+}$	15	35	10	15	<0.04
$[Fe_2O(mtacn)_2(OAc)_2]^{2+}$	30		20	35	<0.04
$[Fe_2O(N3)_2(OBz)_2]^{2+}$		75	35	25	0.08
$[Fe_2O(tpbn)(OAc)_2]_2^{4+}$	45	90	15	50	0.09
$[Fe_2O(tptn)(OAc)_2]_2^{4+}$	50		15	40	<0.04
$[Fe_2O(HBpz_3)_2(OAc)_2]$	160	320	45	70	<0.04
$[Fe_2O(tmip)_2(OPr)_2]^{2+}$	140	380	55		<0.04
Proteins					
oxyhemerythrin (HO_2^-)	570	210	65	30	0.18
methemerythrin (N_3^-)	170	290	310	250	0.27
methemerythrin (SCN^-)	260		470		0.30
methemerythrin (CN^-)	480		240		0.19
methemerythrin (OCN^-)	700	1200	220	90	0.09
ribonucleotide reductase		>205[f]	>40		0.20

[a] Relative scattering intensity calculated from area of ν_s(Fe–O–Fe) per mole of Fe–O–Fe relative to area of $\nu_1(SO_4^{2-})$ per mole of sulfate. Values are ~2× greater than in Figures 4 and 5 due to use of peak areas rather than peak heights. Scattering intensities are accurate to ±20%. [b] Peak area of ν_{as}(Fe–O–Fe) relative to peak area of ν_s(Fe–O–Fe). Intensity ratio was generally independent of excitation wavelength. [c] Values obtained with either 350.7- or 363.8-nm excitation. [d] Values obtained with either 406.7- or 413.1-nm excitation. [e] From ref 34b. [f] Minimum value, owing to photosensitivity, based on two Fe–O–Fe units per met B2 (ref 52). Intensities would be 2-fold greater if there is only one Fe–O–Fe per B2 (ref 53).

In the case of oxyhemerythrin (Figure 5), the enhancement maximum appears to coincide with a major oxo → Fe CT transition (band 3). A similar observation has been reported for chloromethemerythrin.[26] However, this is not the case for the tribridged model complexes (Figure 4) nor for the azido and cyanato derivatives of methemerythrin (Figure 5). All of these systems show at least two enhancement maxima for ν_s(Fe–O–Fe) at ~400 and ~530 nm, which do not correspond to major electronic absorption bands. According to an energy level analysis for Fe–O–Fe complexes, these enhancement maxima may be assigned to additional weakly allowed oxo → Fe(III) CT transitions (bands 4 and 9) that become more important as the bridging angle approaches 90°.[26] The failure of the major oxo → Fe(III) CT bands to promote the intensity of the Fe–O–Fe symmetric stretch in these cases is surprising. A factor that may determine the extent of resonance enhancement associated with a particular oxo → Fe CT transition is the extent of electron delocalization onto the other iron ligands in the electronic excited state. Comparisons of different model complexes (see below) indicate that the presence of unsaturated ligands either cis or trans to the oxo group increases the Raman intensity of the Fe–O–Fe symmetric stretch.

Raman Intensities for ν_s(Fe–O–Fe). In order to quantitate the intensity of the Fe–O–Fe symmetric stretch in proteins and model complexes, molar scattering relative to a sulfate internal standard was determined at four excitation wavelengths (Table III). The

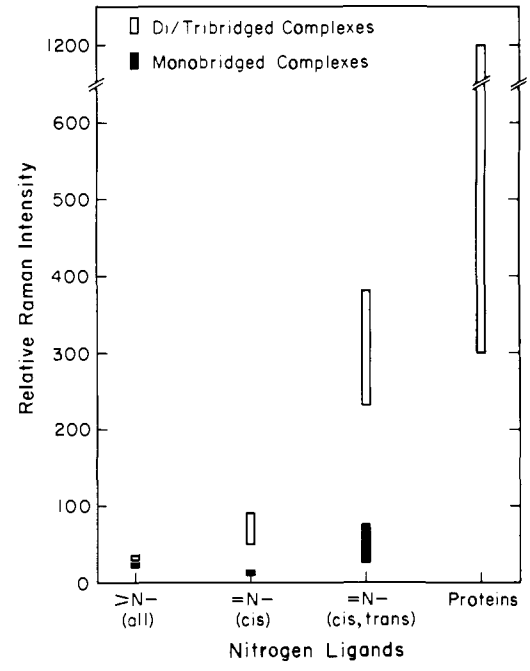

Figure 6. Relationship between the nature of the nitrogenous ligands and the intensity of the Fe–O–Fe symmetric stretch. Data for maximum scattering intensity (peak area) relative to sulfate from Table III. Distribution of ligands cis and trans to oxo group described in text.

values for the model compounds were obtained on samples in the solid state, whereas the protein data were obtained on aqueous samples at 4 °C. Few of the model compounds are stable enough in aqueous solution to be able to determine the effect of dissolution on their scattering intensities relative to sodium sulfate. Freezing improves the stability of aqueous samples, but the differential dispersion of solutes makes intensity ratios inaccurate.[31] In a previous study of the oxo-bridged ruthenium dimer, $K_4[ORu_2Cl_{10}]$, it was found that the scattering intensity at the enhancement maximum was essentially the same for solid and aqueous states.[45] The $[Fe_2O(tacn)_2(OAc)_2]^{2+}$ complex has been reported to be stable in aqueous solution for up to 1 h.[35] Raman spectra recorded within this time period revealed that the ν_s(Fe–O–Fe) mode shifted to 523 cm^{-1} but maintained a relative molar intensity of 15, the same value as observed in the solid state with 514.5-nm excitation (Table III).

For all of the compounds in Table III the symmetric Fe–O–Fe mode produces Raman scattering that is at least 5-fold more intense on a molar basis than the ν_1 mode of sulfate. The variation in relative scattering intensity with excitation wavelength demonstrates that this enhanced scattering is due to the resonance Raman effect. Furthermore, in almost all cases the ν_s(Fe–O–Fe) modes are more strongly enhanced with near-UV (364, 410 nm) excitation than with visible (458, 514 nm) excitation. Thus, the occurrence of a stronger ν_s(Fe–O–Fe) enhancement maximum in the near-UV region (as in Figures 4 and 5) appears to be a general characteristic of oxo-bridged dinuclear iron clusters.

Despite the above similarities, the actual magnitude of the ν_s(Fe–O–Fe) Raman intensity is surprisingly variable. Maximum scattering intensities for most of the model compounds range from 25 to 90, whereas those for the dinuclear iron proteins range from 300 to 1200. Only the tribridged $HBpz_3$ and tmip complexes, with their maximal scattering intensities of 320 and 380, respectively, are within the range observed for the proteins. It would appear that the nature of the other ligating groups has a considerable effect on the degree of scattering by the Fe–O–Fe moiety. Factors which appear to *enhance* the intensity of the ν_s(Fe–O–Fe) mode are (1) the presence of multiple bridging groups and the resulting decrease in Fe–O–Fe angle, (2) the presence of unsaturated nitrogen ligands, and (3) especially the presence of unsaturated nitrogen ligands *trans to the oxo bridge*. The relative influence of these three factors is presented graphically in Figure 6. In

contrast, the intensity of the ν_s(Fe–O–Fe) mode appears to be depressed by phenolate ligands and by extreme asymmetry in the environments of the two iron atoms.

The monobridged complexes in this investigation with their large Fe–O–Fe angles (>150°) had fairly low ν_s(Fe–O–Fe) scattering intensities. The values for the Cl-pdc and hedta complexes (maximum of 25) are typical. The poor scattering in these two complexes as well as in $[Fe_2OCl_6]^{2-}$ and μ-oxo-bridged complexes with salicylaldimine-type ligands has been reported previously.[34] For the *n*-propsal complex, which is in the salicylaldimine category, the even lower scattering intensity (i.e., 10) may be ascribed to the presence of phenolate ligands. The tetranuclear mhxta complex with the equivalent of only one phenolate ligand per two Fe reaches slightly higher intensities (i.e., 20). More intense scattering was observed with the phen ligand (maximum of 75) which has unsaturated nitrogens both cis and trans to the oxo group. The Cl-pdc complex which also has unsaturated nitrogen ligands trans to the oxo group showed no such enhancement, possibly due to the effect of electron-withdrawing substituents on the aromatic ring. The asymmetric $[(N5)Fe–O–Fe(X)_3]^+$ complexes, with X = Cl or Br and a saturated N in the trans position, exhibited exceedingly weak Fe–O–Fe scattering (i.e., 5) which appears to be related to the marked inequivalence of the coordination environments of the two iron atoms.[14b]

In the dibridged category, the hdp complexes have two pyridines and one phenolate per Fe with a saturated amine trans to the oxo group.[21] These exhibit intermediate scattering intensities (maximum of 50–70), consistent with the presence of unsaturated ligands in the cis position. The shifting of the excitation maximum from the 410- to the 360-nm region is unique among the dinuclear iron model compounds and may be due to the influence of the phenolate ligands. The tpa complexes have three pyridine ligands that are arranged asymmetrically about the two iron atoms, resulting in one iron having a pyridine and the other iron having a saturated amine in the position trans to the oxo group.[20a] These complexes have increased scattering intensities relative to the hdp complexes due to the presence of this trans pyridine ligand. The enhancement values in the benzoate- and acetate-bridged complexes (i.e., 140–160) are actually lower estimates because the ν_s(Fe–O–Fe) mode occurs as a Fermi resonance doublet and only the stronger of the two peaks was used for the intensity calculation.[20b] The phosphate-bridged tpa complex has only a single strong peak in the ν_s(Fe–O–Fe) region, and its larger enhancement (maximum of 230) is likely to be a more accurate measure of the contribution of a trans pyridine to the Fe–O–Fe scattering intensity. The fact that the dibridged $[Fe_2O(tpa)_2(O_2PR_2)]^{3+}$ complex exhibits a 3-fold greater enhancement than the monobridged $[Fe_2O(phen)_4(H_2O)_2]^{4+}$ complex with only a 17° decrease in Fe–O–Fe angle (from 155° to 138°) suggests that the presence of an additional bridging group may be a more important factor than the decrease in Fe–O–Fe angle.

For the tribridged complexes, the lowest scattering intensity (maximum of 35) is found for the tacn-based species, which have only saturated amine ligands. This is still an ~2-fold greater enhancement than is found in monobridged complexes with a similar set of ligands. The ~2- to 3-fold higher intensities for the N3, tpbn, and tptn complexes (i.e., 50–90) appear to be related to the presence of two unsaturated nitrogen ligands (benzimidazole or pyridine) per Fe located cis to the oxo group. Each of these complexes has saturated amines in the trans position.[14c,18] Finally, an additional ~3- to 8-fold enhancement is observed for the $HBpz_3$ and tmip complexes (i.e., 320–380), that have three unsaturated nitrogen ligands (pyrazoles or imidazoles) per Fe with two per cluster being located trans to the oxo bridge. The values for the $HBpz_3$ and tmip complexes fall within the range for the dinuclear iron proteins and demonstrate the importance of a multi-bridged structure and of trans unsaturated nitrogen ligands, in particular, for achieving large resonance enhancements of the Fe–O–Fe stretch.

In hemerythrin where maximum scattering intensities typically vary from 310 to 570, one of the iron atoms is ligated to a cis and a trans imidazole, while the other iron atom is ligated to two cis and one trans imidazoles.[5] Addition of another unsaturated ligand such as cyanate in a position cis to the oxo group results in a further substantial increase in Fe–O–Fe intensity to 1200. The large scattering intensity for the ν_s(Fe–O–Fe) mode in ribonucleotide reductase (maximum >205) indicates that the dinuclear iron center in this protein is multiply bridged, with imidazole ligands located trans to the oxo group. The relatively low value suggests the absence of imidazole ligands cis to the oxo group.

Raman Intensities for ν_{as}(Fe–O–Fe). The asymmetric Fe–O–Fe stretching vibration generally occurs as a strong feature in the infrared spectrum and as a weak to nonobservable feature in the Raman spectrum. However, there are several cases among the dinuclear iron model complexes and proteins in which the ν_{as}(Fe–O–Fe) mode achieves unusually high Raman intensity. Quantitation of the peak area for the ν_{as} mode relative to the peak area for the ν_s(Fe–O–Fe) mode is reported in Table III. In symmetrically coordinated complexes, the I_{as}/I_s ratio tends to have a maximum value of 0.2 for the monobridged clusters and 0.1 for the di- and tribridged clusters. A dramatic deviation is observed for the asymmetrical $[(N5)Fe–O–Fe(X)_3]^+$ complexes with I_{as}/I_s ratios of 2.4 (X = Br) and 4.2 (X = Cl). The difference in the Fe–O bond lengths is only 0.07 Å for the Br complex and 0.03 Å for the chloride complex (Table I). The other monobridged complex with a sizable I_{as}/I_s ratio is $Fe_2O(n\text{-propsal})_4$ with a value of 0.5. In this case asymmetry is introduced by the ligand sets on each iron being staggered by 90° with respect to one another.[11] These results indicate that the increased scattering intensity of ν_{as}(Fe–O–Fe) is primarily due to differences in the ligand environments of the iron atoms.

The I_{as}/I_s ratio in these complexes is relatively unaffected by excitation wavelength, implying that both ν_s and ν_{as} modes are in resonance with the same oxo → Fe chromophores. The unusually low value for the intensity of the ν_s(Fe–O–Fe) mode relative to sulfate in the $[Fe_2O(N5)Cl_3]^+$ complex (i.e., value of 5 in Table III) suggests that the large value for I_{as}/I_s is due to a depression of ν_s intensity as well as an enhancement of ν_{as} intensity. Since asymmetric stretching modes gain intensity via *B*-term rather than *A*-term scattering,[43a] they have a different dependence on the electronic transition moment of the chromophore and, thus, may exhibit different resonance enhancement behavior.

The dibridged tpa complexes also show unusually high I_{as}/I_s ratios of ~0.2–0.3,[20b] particularly compared to the values of 0.09 or less for the tribridged complexes. The $[Fe_2O(tpa)_2(OBz)]^{3+}$ and $[Fe_2O(tpa)_2\{O_2P(OPh)_2\}]^{3+}$ complexes are known to have an unsymmetrical arrangement of pyridine and amine ligands with respect to the dinuclear iron cluster[20] and differences of 0.03 Å and 0.04 Å, respectively, in the Fe–μO bond lengths (Table I). The $[Fe_2O(tpa)_2(OAc)]^{3+}$ complex has a similarly unsymmetrical arrangement of ligands,[20a] but a variation of only 0.01 Å in Fe–O bond distances. Several forms of hemerythrin also seem to have enhanced intensity ratios (i.e., 0.2–0.3) compared to those observed for the tribridged complexes. This is in agreement with the known asymmetry arising from the presence of an exogenous ligand binding site on only one of the two iron atoms. However, the reported 0.25-Å difference in Fe–O bond lengths in an X-ray crystallographic study of azidomethemerythrin[5a] is probably an overestimate. Such an extreme asymmetry would be expected to depress the intensity of ν_s(Fe–O–Fe) and yield a considerably larger value for I_{as}/I_s. Furthermore, investigations of azidomethemerythrin by X-ray absorption[32,54] and Mössbauer spectroscopy[4] show no indication of such a wide spread in Fe–O distances, and the same is true from the crystal structure of azidomet*myo*hemerythrin.[5b] The I_{as}/I_s ratio of 0.2 for ribonucleotide reductase is similar to that observed for hemerythrin and is thus indicative of some asymmetry in ligand distribution

(52) Lynch, J. B.; Juarez-Garcia, C.; Münck, E.; Que, L., Jr. *J. Biol. Chem.* **1989**, *264*, 8091.
(53) Sahlin, M.; Ehrenberg, A.; Gräslund, A.; Sjöberg, B.-M. *J. Biol. Chem.* **1986**, *261*, 2778.
(54) Zhang, K.; Stern, E. A.; Ellis, F.; Sanders-Loehr, J.; Shiemke, A. K. *Biochemistry* **1988**, *27*, 7470.

at its dinuclear iron site, as has been suggested by Mössbauer spectroscopic studies.[55]

General Characteristics of the Fe–O–Fe Moiety. Oxo-bridged dinuclear iron centers exhibit a wide variability in their Fe–O–Fe bond angles (120° to 180°), the number of additional bridging groups (0 to 2), and the types of ligands which support dimerization. Previous studies have indicated that these three parameters have very little influence on the characteristics of the dinuclear iron site. In most of these compounds the Fe–O bond lengths are near 1.80 Å and the antiferromagnetic coupling constants ($-J$) are close to 100 cm^{-1}.[2,56] In addition, the electronic spectra (Table II) are strikingly similar, with several intense bands between 300 and 380 nm and a series of weaker transitions between 400 and 500 nm.[26,49] One technique that is sensitive to the structural diversity of Fe–O–Fe complexes is vibrational spectroscopy. The frequencies of the symmetric and asymmetric Fe–O–Fe stretches are sensitive indicators of Fe–O–Fe bond angle (Figure 2). Furthermore, the extent of resonance Raman enhancement of the symmetric stretch appears to be related to the presence of additional bridging groups as well as to the nature of the nonbridging ligands.

Resonance Raman intensities for symmetric vibrations are expected to be proportional to ϵ^2, where ϵ is the molar absorptivity of the electronic transition responsible for resonance enhancement.[43,57] Raman excitation profiles (Figures 4 and 5) for the ν_s(Fe–O–Fe) mode appear to correspond to minor oxo → Fe CT bands rather than to the major electronic transitions in the near-UV region. Further evidence for this viewpoint is that the >100-fold variation in ν_s(Fe–O–Fe) molar intensities relative to sulfate (Table III) is not matched by a 10-fold variation in the molar absorptivities of the major near-UV bands. This would argue against the mismatch in the absorption and excitation profiles being simply the result of a resonance Raman interference phenomenon.[48] In contrast, the minor oxo → Fe(III) CT components in the optical spectrum do appear to vary in a manner consistent with the observed Raman intensities. Thus, for example, the tribridged $HBpz_3$ complex has an ~10-fold greater ν_s(Fe–O–Fe) enhancement than the tribridged tacn complex and an ~3-fold greater molar absorptivity in the 390–400-nm region (Figure 4).

In the resonance Raman effect, vibrational intensities are governed by the extent of nuclear displacement in the electronic excited state.[43] The present study of Fe–O–Fe complexes has pointed to a correlation between the presence of unsaturated nitrogen ligands and resonance enhancement of ν_s(Fe–O–Fe). In this case it is likely that unsaturated ligands such as pyridine, pyrazole, and imidazole increase the delocalization of charge between the oxo group and the iron complex and thereby increase the vibrational intensity of the Fe–O–Fe mode. Such π-acceptor ligands would be expected to facilitate delocalization since the oxo → Fe CT transition appears to originate from π-symmetry orbitals.[26] A particularly dramatic example is the 11-fold increase in maximum scattering intensity of the tribridged complexes upon replacement of the saturated tacn ligand with the imidazole-containing tmip ligand (Table III). A similar trend has been observed for ν(Mo=O) and ν(Mo—Cl) in $LMoOCl_2$ complexes, where the Raman intensities for L = tris[1-(3,5-dimethylpyrazolyl)]borate are 6- to 10-fold greater than for L = mtacn.[58] Another example of ligand effects is the 3- to 4-fold increase in the ν_s(Fe–O–Fe) intensity for the cyanato form of methemerythrin relative to the cyano and azido derivatives (Table III). In an analogous fashion, the Ru–O–Ru vibration in $[ORu_2Cl_{10}]^{4-}$ undergoes a 5-fold increase in enhancement when the chloride ligands are replaced by bromides.[45]

Although ν_s(Fe–O–Fe) enhancements are observed with unsaturated ligands located either cis or trans to the oxo group, the enhancements appear to be more pronounced for the trans arrangement. Thus, the greatest ν_s(Fe–O–Fe) relative intensities (i.e., >150) are observed for the dibridged tpa complexes with one trans pyridine, the tribridged $HBpz_3$ complex with two trans pyrazoles, and the hemerythrin and tribridged tmip complexes with two trans imidazoles. The Fe–O–Fe symmetric stretch of ribonucleotide reductase with its relative scattering intensity >205 falls into this same high-intensity range. These data suggest that ribonucleotide reductase has at least one histidine per iron atom (as has also been proposed from NMR experiment[53]) and that these histidines are likely to be oriented trans to the bridging oxo group.

In the case of the dinuclear iron protein purple acid phosphatase (and, similarly, uteroferrin), resonance Raman spectra have failed to reveal any ^{18}O-sensitive modes that could be attributed to an Fe–O–Fe vibration.[8] An Fe–O–Fe peak with a scattering intensity less than 40 would be difficult to detect by resonance Raman spectroscopy with the presently available protein concentrations (<5 mM). The presumed Fe–O–Fe center in these proteins is, therefore, behaving quite differently from hemerythrin and ribonucleotide reductase and more like a number of the typical oxo-bridged model compounds. This protein also lacks significant electronic absorption bands between 350 and 420 nm. Other spectroscopic investigations indicate that purple acid phosphatase has a multibridged dinuclear iron cluster with one or more tyrosinate ligands and at least one histidine per iron.[4,8,59] There are several factors which could account for the failure to observe an Fe–O–Fe mode in this protein: (1) the presence of a tyrosinate ligand depresses ν_s(Fe–O–Fe) intensities or shifts the enhancement maximum to higher energy as in the phenolate-containing *n*-propsal, mhxta, and hdp model complexes; (2) the unsymmetrical distribution of tyrosinate ligands with respect to the two iron atoms leads to a low ν_s(Fe–O–Fe) intensity as in the $[(N5)Fe–O–Fe(X)_3]^+$ complexes; and (3) in contrast to hemerythrin and ribonucleotide reductase, the histidine ligands in purple acid phosphatase are located in positions cis rather than trans to the μ-oxo bridge.

Acknowledgment. We are grateful to Drs. Harry B. Gray, Edward I. Solomon, and Thomas G. Spiro for helpful discussions, Salman Ahmad for obtaining excitation data on cyanatomethemerythrin, and Madeline Dalrymple for quantitating Raman intensities. We also thank Drs. Geoffrey B. Jameson, Donald M. Kurtz, Jr., Stephen J. Lippard, Lawrence Que, Jr., Harvey J. Schugar, Hans Toftlund, and Karl Wieghardt for providing samples of dinuclear iron model compounds. This work was supported by National Institutes of Health Grant GM 18865 (T.M.L. and J.S.-L.) and Grant GM 32117 (B.A.A.).

(55) Atkin, C. L.; Thelander, L.; Reichard, P.; Lang, G. *J. Biol. Chem.* **1973**, *248*, 7464.
(56) Thich, J. A.; Toby, B. H.; Powers, D. A.; Potenza, J. A.; Schugar, H. J. *Inorg. Chem.* **1981**, *20*, 3314.
(57) Blair, D. F.; Campbell, G. W.; Schoonover, J. R.; Chan, S. I.; Gray, H. B.; Malmström, B. G.; Pecht, I.; Swanson, B. I.; Woodruff, W. H.; Cho, W. K.; English, A. M.; Fry, H. A.; Lum, V.; Norton, K. A. *J. Am. Chem. Soc.* **1985**, *107*, 5755.
(58) Backes, G.; Enemark, J. H.; Loehr, T. M., unpublished results.
(59) Scarrow, R. C.; Pyrz, J. W.; Que, L., Jr. *J. Am. Chem. Soc.*, in press.